

Alcohol and secondary amine complexes of tri-*tert*-butylaluminium: enhanced stability through intramolecular hydrogen bonding †

C. Niamh McMahon,^a Simon G. Bott^{*,b} and Andrew R. Barron^{*,a}

^a Department of Chemistry, Rice University, Houston, TX 77005, USA

^b Department of Chemistry, University of Houston, Houston, TX 77204, USA

Reaction of $\text{Al}(\text{Bu}^t)_3$ with between 1 and 2 equivalents of $\text{HOCH}_2\text{CH}_2\text{CH}_2\text{NMe}_2$ allows for the isolation of the Lewis acid–base complex, $(\text{Bu}^t)_3\text{Al}[\text{O}(\text{H})\overline{\text{CH}_2\text{CH}_2\text{CH}_2\text{NMe}_2}]$ **1**, which undergoes alkane elimination above 45 °C to yield $[(\text{Bu}^t)_2\text{Al}(\mu\text{-OCH}_2\text{CH}_2\text{CH}_2\text{NMe}_2)]_2$ **2**. Compound **2** is also formed directly when 2 equivalents of $\text{Al}(\text{Bu}^t)_3$ react with 1 equivalent of $\text{HOCH}_2\text{CH}_2\text{CH}_2\text{NMe}_2$. The molecular structure of **1** shows an Al–O bond distance comparable to that found in the bridging alkoxide compounds **2** and $[(\text{Bu}^t)_2\text{Al}(\mu\text{-OPr}^n)]_2$ **3**, suggesting that the Al–O···H unit may be considered analogous to a bridging alkoxide unit, $\text{Al}(\mu\text{-OR})\text{Al}$, as a consequence of a significant contribution from the zwitterionic alkoxide[−]/ammonium⁺ form made possible by a strong intraligand hydrogen bond. The kinetics of the conversion of **1** into **2** have been studied. A large activation energy and positive deuterium isotope effect are consistent with breaking of the hydrogen bond during the transition state. The reaction of $(\text{Bu}^t)_3\text{Al}(\text{NMe}_2)$ **4** with ethanol yields $[(\text{Bu}^t)_2\text{Al}(\mu\text{-OEt})]_2$ **5**. The reaction of $\text{Al}(\text{Bu}^t)_3$ with $\text{HN}(\text{Me})(\text{CH}_2)_n\text{NMe}_2$ ($n = 3$ or 2) yields the stable Lewis acid–base adducts $(\text{Bu}^t)_3\text{Al}[\text{NH}(\text{Me})\overline{\text{CH}_2\text{CH}_2\text{CH}_2\text{NMe}_2}]$ **6** and $(\text{Bu}^t)_3\text{Al}[\text{NH}(\text{Me})\overline{\text{CH}_2\text{CH}_2\text{NMe}_2}]$ **7**, respectively. The molecular structures of compounds **1–3**, **6** and **7** have been confirmed by X-ray crystallography. The implications of the structures and stabilities of compounds **1**, **6** and **7** are discussed with respect to the protonolysis reaction of aluminium alkyls with Brønsted acids (HX) and a new intermolecular elimination mechanism is proposed.

The reaction of an aluminium alkyl (AlR_3) with a weak Brønsted acid (HX, *e.g.* HOR, HNR_2 , *etc.*), resulting in alkane elimination [equation (1)], is ubiquitous in the organometallic

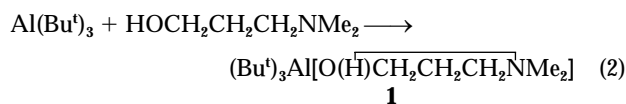


chemistry of aluminium.¹ In general this reaction is very facile and is proposed to occur *via* an intermediate Lewis acid–base complex, *i.e.* $\text{AlR}_3(\text{HX})$. While such alkyl complexes with oxygen Brønsted acids (*e.g.* H_2O , HOR, HO_2CR , *etc.*) are unstable, precluding isolation, they have been observed spectroscopically at low temperature,² and the aryl derivatives are more stable.³ In contrast, there have been few key examples of stable amine complexes reported. Stable water co-ordination compounds have been isolated in a similar manner for gallium³ and aluminium siloxides.⁴ Oliver and co-workers⁵ have shown that subtle variations in the reaction conditions, or the purity of the reactants, can allow for the isolation of trialkyl aluminium complexes of thiomorpholine in the absence of hydrogen bonding, presumably as a result of subtle kinetic stabilization effects. We have shown that stable Lewis acid–base complexes between aluminium alkyls and primary and secondary amines may be isolated if at least one heteroatom donor ligand is already present on aluminium, *e.g.* $\text{AlR}_n(\text{OR})_{3-n}(\text{HNR}_2)$ where $n = 1$ or 2 .⁶ Based upon spectroscopic data we have proposed that the presence of a heteroatom donor ligand (*e.g.*, alkoxide, aryloxide, amide, *etc.*) significantly reduces the basicity of the aluminium alkyl group as a result of high electronegativity at the aluminium atom.⁷ While these complexes appear to be special cases of stability, Robinson *et al.*⁸ have reported that the cyclic secondary amine, 1,4,8,11-tetraazacyclotetradecane ([14]aneN₄), forms a stable adduct with AlMe_3 , as a consequence of the intramolecular hydrogen bonding between the N–H of the nitrogen co-ordinated to aluminium and an

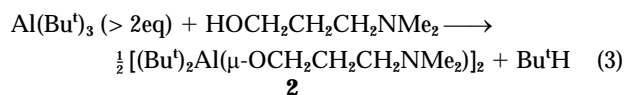
adjacent uncomplexed nitrogen center. Although, the generality of this approach is unknown, the isolation of stable secondary amine complexes of aluminium trialkyls through the use of strong intramolecular hydrogen-bonded ligands suggests that a similar approach should be successful in the isolation of alcohol complexes of AlR_3 . In this regard we have investigated the reaction of $\text{Al}(\text{Bu}^t)_3$ with 3-dimethylamino-1-propanol ($\text{HOCH}_2\text{CH}_2\text{CH}_2\text{NMe}_2$).

Results and Discussion

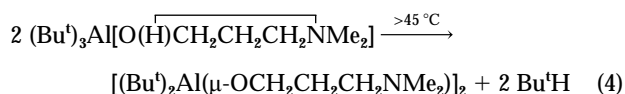
Reaction of $\text{Al}(\text{Bu}^t)_3$ with between 1 and 2 equivalents of $\text{HOCH}_2\text{CH}_2\text{CH}_2\text{NMe}_2$ allows for the isolation of the Lewis acid–base complexes, $(\text{Bu}^t)_3\text{Al}[\text{O}(\text{H})\overline{\text{CH}_2\text{CH}_2\text{CH}_2\text{NMe}_2}]$ **1**, equation (2); if a less than stoichiometric amount of $\text{HOCH}_2\text{CH}_2\text{CH}_2\text{NMe}_2$



$\text{CH}_2\text{CH}_2\text{NMe}_2$ is employed then both compound **1** and $[(\text{Bu}^t)_2\text{Al}(\mu\text{-OCH}_2\text{CH}_2\text{CH}_2\text{NMe}_2)]_2$ **2** may be observed in the reaction mixture by ¹H NMR spectroscopy. The exclusive formation of compound **2** is observed if 2 equivalents (eq) of $\text{Al}(\text{Bu}^t)_3$ are reacted with $\text{HOCH}_2\text{CH}_2\text{CH}_2\text{NMe}_2$, equation (3).



Compound **1** is stable with respect to alkane elimination at room temperature as a solid or in solution, however, heating a benzene solution above 45 °C results in its slow (*ca.* 12 h), but stoichiometric, conversion to compound **2** [equation (4)].



† Dedicated to the memory of Geoffrey Wilkinson for his inspiration, encouragement and support.

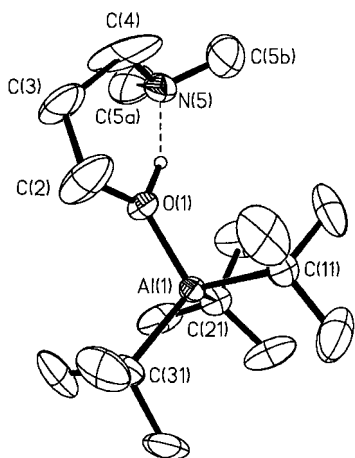


Fig. 1 Molecular structure of $(\text{Bu})_3\text{Al}[\text{O}(\text{H})\text{CH}_2\text{CH}_2\text{CH}_2\text{NMe}_2]$ **1**. Thermal ellipsoids shown at the 30% level, and hydrogen atoms bonded to carbon are omitted for clarity

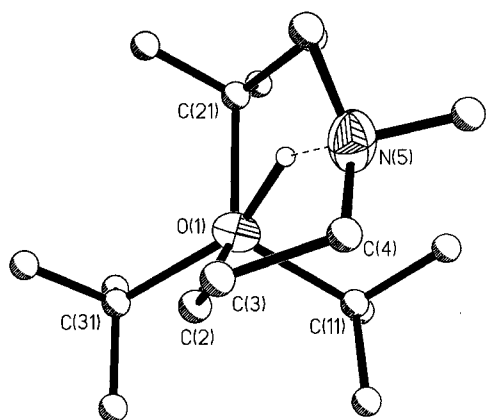


Fig. 2 Structure of $(\text{Bu})_3\text{Al}[\text{O}(\text{H})\text{CH}_2\text{CH}_2\text{CH}_2\text{NMe}_2]$ **1** viewed along the $\text{Al}(1)\text{--O}(1)$ vector. Carbon atoms are shown as shaded spheres and hydrogen atoms bonded to carbon are omitted for clarity

Table 1 Selected bond lengths (Å) and angles (°) in $(\text{Bu})_3\text{Al}[\text{O}(\text{H})\text{CH}_2\text{CH}_2\text{CH}_2\text{NMe}_2]$ **1**

$\text{Al}(1)\text{--O}(1)$	1.815(5)	$\text{Al}(1)\text{--C}(11)$	2.028(8)
$\text{Al}(1)\text{--C}(21)$	2.021(9)	$\text{Al}(1)\text{--C}(31)$	2.034(9)
$\text{O}(1)\text{--C}(1)$	1.38(1)		
$\text{O}(1)\text{--Al}(1)\text{--C}(11)$	104.6(3)	$\text{O}(1)\text{--Al}(1)\text{--C}(21)$	101.9(3)
$\text{O}(1)\text{--Al}(1)\text{--C}(31)$	109.0(3)	$\text{C}(11)\text{--Al}(1)\text{--C}(21)$	113.7(4)
$\text{C}(11)\text{--Al}(1)\text{--C}(31)$	112.8(4)	$\text{C}(21)\text{--Al}(1)\text{--C}(31)$	113.6(4)

Compounds **1** and **2** have been spectroscopically characterized (see Experimental section) and their molecular structures have been determined by X-ray crystallography. Attempts to isolate the methyl, ethyl or isobutyl analogs of compound **1** have been unsuccessful.

The molecular structure of $(\text{Bu})_3\text{Al}[\text{O}(\text{H})\text{CH}_2\text{CH}_2\text{CH}_2\text{NMe}_2]$ **1** is shown in Fig. 1; selected bond lengths and angles are given in Table 1. Based upon the relative basicity of alcohols and tertiary amines,⁹ co-ordination of the $\text{HOCH}_2\text{CH}_2\text{CH}_2\text{NMe}_2$ ligand may be expected to be *via* the nitrogen, as is seen in $\text{Me}_3\text{Ga}(\text{NH}_2\text{CH}_2\text{CH}_2\text{OMe})$.¹⁰ However, as can be seen from Fig. 1 complexation occurs through the oxygen, O(1). Such a co-ordination is presumably as a consequence of the strong hydrogen-bond interaction 'tying-up' the amine's lone pair. As we have previously observed for phosphine complexes of aluminium trialkyls^{11,12} the alcohol substituents are staggered [$\text{C}(31)\text{--Al}(1)\text{--O}(1)\text{--C}(2) = 31^\circ$] with respect to the aluminium substituents, see Fig. 2. The co-ordination geometry about the

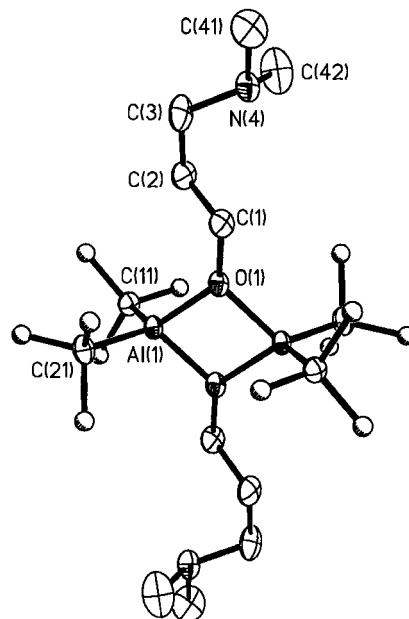


Fig. 3 Molecular structure of $[(\text{Bu})_2\text{Al}(\mu\text{-OCH}_2\text{CH}_2\text{CH}_2\text{NMe}_2)]_2$ **2**. Thermal ellipsoids shown at the 20% level. The methyl carbon atoms of the *tert*-butyl groups are shown as shaded spheres and all hydrogen atoms are omitted for clarity

Table 2 Selected bond lengths (Å) and angles (°) in $[(\text{Bu})_2\text{Al}(\mu\text{-OCH}_2\text{CH}_2\text{CH}_2\text{NMe}_2)]_2$ **2**

$\text{Al}(1)\text{--O}(1)$	1.848(2)	$\text{Al}(1)\text{--O}(1a)$	1.862(2)
$\text{Al}(1)\text{--C}(11)$	2.008(4)	$\text{Al}(1)\text{--C}(21)$	2.003(4)
$\text{O}(1)\text{--C}(1)$	1.445(4)		
$\text{O}(1)\text{--Al}(1)\text{--O}(1a)$	78.81(6)	$\text{O}(1)\text{--Al}(1)\text{--C}(11)$	117.0(1)
$\text{O}(1)\text{--Al}(1)\text{--C}(21)$	113.6(1)	$\text{C}(11)\text{--Al}(1)\text{--C}(21)$	117.2(1)
$\text{Al}(1)\text{--O}(1)\text{--Al}(1a)$	101.19(9)	$\text{Al}(1)\text{--O}(1)\text{--C}(2)$	131.9(2)

aluminium is comparable to other Lewis base complexes of $\text{Al}(\text{Bu})_3$ that we have reported.^{12,13} However, the $\text{Al}(1)\text{--O}(1)$ bond distance [1.815(5) Å] is atypical of an ether-like $\text{Al}\text{--O}$ interaction (1.90–2.02 Å), and is within the range expected for a bridging alkoxide (1.76–1.86 Å¹⁴), see below. The hydrogen atom was located in the electron difference map. The $\text{O}(1)\text{--H}(1)$ distance (1.27 Å) is significantly longer, and $\text{N}(5)\text{--H}(1)$ (1.47 Å) shorter, than has been observed for hydrogen bonded aluminium and gallium hydroxides.^{15,16} In addition, the $\text{O}(1)\text{--H}(1)$ distance is shorter than observed for ketone complexes or trialkylammonium salts, $\text{R}_3\text{NH}^+ \cdots \text{O}=\text{CR}_2$ (1.72–1.94 Å).¹⁷

The dimeric alkoxide bridged structure of $[(\text{Bu})_2\text{Al}(\mu\text{-OCH}_2\text{CH}_2\text{CH}_2\text{NMe}_2)]_2$ **2** has been confirmed by X-ray crystallography and is shown in Fig. 3; selected bond lengths and angles are given in Table 2. The structure consists of a discrete centrosymmetric alkoxide bridged dimer. The amine residues show neither intra- or inter-molecular association with aluminium. In fact in compound **2** the amine's lone pair is directed away from the aluminium centers. The bond lengths and angles within the Al_2O_2 core are within the range expected^{14,18} and are similar to those in $[(\text{Bu})_2\text{Al}(\mu\text{-OPr}^n)]_2$ **3**. Compound **3** is isolated from the reaction of $\text{Al}(\text{Bu})_3$ with HOPr^n (see Experimental section) and its molecular structure is shown in Fig. 4; selected bond lengths and angles are given in Table 3. The two $\text{Al}\text{--O}$ distances to each oxygen in both compound **2** and **3** are, within experimental error, the same. This suggests the presence of symmetrically bridging alkoxide ligands in both, as is commonly observed for the group 13 elements.¹⁹ The lack of intra-molecular co-ordination by the amine residue in compound **2** is presumably due to the steric repulsion that would be experienced between eclipsed *tert*-butyl and methyl groups upon the formation of an $\text{Al}\text{--N}$ bond.

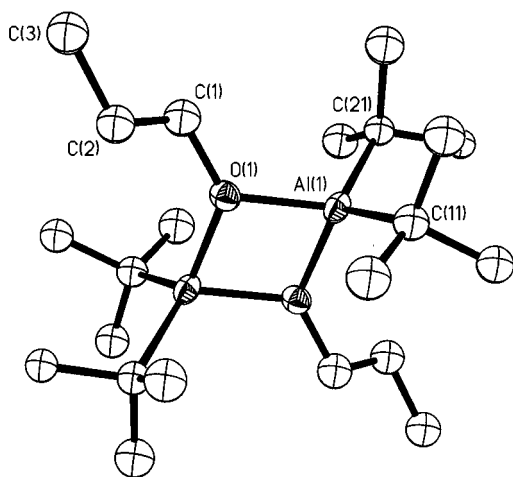


Fig. 4 Molecular structure of $[(\text{Bu}^t)_2\text{Al}(\mu\text{-OPr}^m)]_2$ **3**. Thermal ellipsoids shown at the 30% level, and hydrogen atoms are omitted for clarity

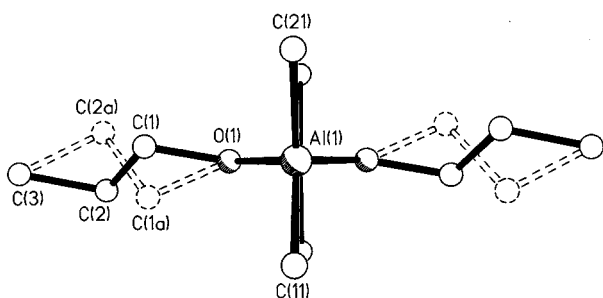


Fig. 5 Partial co-ordination sphere of Al(1) in $[(\text{Bu}^t)_2\text{Al}(\mu\text{-OPr}^m)]_2$ **3** viewed along the Al(1) \cdots Al(1a) vector, showing the disordered *n*-propoxide ligands. Hydrogen atoms and the *tert*-butyl methyl groups have been omitted for clarity

Table 3 Selected bond lengths (Å) and angles (°) in $[(\text{Bu}^t)_2\text{Al}(\mu\text{-OPr}^m)]_2$ **3**

Al(1)–O(1)	1.855(9)	Al(1)–O(1a)	1.843(9)
Al(1)–C(11)	1.94(2)	Al(1)–C(21)	2.03(2)
O(1)–C(1)	1.47(2)		
O(1)–Al(1)–O(1a)	78.6(2)	O(1)–Al(1)–C(11)	114.6(6)
O(1)–Al(1)–C(21)	114.0(5)	C(11)–Al(1)–C(21)	114.6(6)
Al(1)–O(1)–Al(1a)	101.4(4)	Al(1)–O(1)–C(1)	125.3(9)

The structure of compound **3** shows crystallographic disorder of two distinct classes. First, as we have previously observed²⁰ the *tert*-butyl groups exhibit rotational disorder about their respective Al–C_α bonds. Second, the O(1)–C(1)–C(2)–C(3) linkage shows severe disorder such that C(1) and C(2) are positioned on opposite sides of the plane defined by Al(1), O(1) and C(3), Fig. 5. Thus, the *n*-propoxide ligand makes a Z shape between O(1) and C(3), in which the rigid ends of the *n*-propoxide chain are fixed in space by molecular packing forces, leaving the interior link to adopt multiple orientations: the so-called ‘slinky’ effect.²¹

Alkoxide[−]/ammonium⁺ zwitterion versus alcohol/tertiary amine

Although the preference for co-ordination of the 3-dimethylamino-1-propanol *via* the alcohol oxygen, rather than the amine nitrogen, could be a consequence of steric hindrance at the amine, the isolation and stability of $(\text{Bu}^t)_3\text{Al}(\text{NMe}_3)$ **4** (see Experimental section) is counter to this reasoning. Furthermore, the structural characterization of $(\text{Bu}^t)_3\text{AlP}(\text{Pr}^m)_3$ and $[\text{AlCl}(\text{Bu}^t)_3]^-$ has shown that the geometry about the ‘ $(\text{Bu}^t)_3\text{Al}$ ’ moiety is essentially independent of the steric hindrance of a

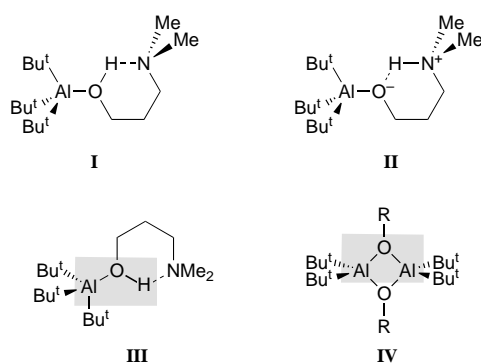


Table 4 Selected kinetic data for the alkane elimination reaction of $(\text{Bu}^t)_3\text{Al}[\text{O}(\text{H})\text{CH}_2\text{CH}_2\text{CH}_2\text{NMe}_2]^a$

T/K	$10^4 k_1^b \text{ s}^{-1}$
318	0.172
326	0.608
333	1.279
340	5.041

^a From ¹H NMR spectra measured in C₆D₆. ^b 0.132 M solution of $(\text{Bu}^t)_3\text{Al}[\text{O}(\text{H})\text{CH}_2\text{CH}_2\text{CH}_2\text{NMe}_2]$.

co-ordinated Lewis base.^{12,13} Thus, co-ordination of HOCH₂–CH₂CH₂NMe₂ to aluminium *via* oxygen rather than nitrogen, suggests that the alcohol hydrogen atom is a stronger Lewis acid than the aluminium. It is commonly observed that the acidity of water increases when complexed to a transition metal.²² Thus, it is reasonable that the pK_a of the alcohol also changes upon co-ordination to aluminium, and in the presence of an intramolecular Lewis base, a strong hydrogen bond/proton transfer to the amine results. Likewise, the unusually short Al–O bond length in the structure of compound **1** suggests that instead of the alcohol/tertiary amine form (**I**) the zwitterionic alkoxide[−]/ammonium⁺ form (**II**) may be considered. If the structure of **1** has a significant contribution from the latter structure then it is possible to consider compound **1** as an isolobal analog of a bridging alkoxide compound.²³ In particular, the Al(1)–O(1)–H(1) unit (see **III**) may be considered analogous to a bridging alkoxide unit, Al(μ-OR)Al (**IV**), as observed in $[(\text{Bu}^t)_2\text{Al}(\mu\text{-OCH}_2\text{CH}_2\text{CH}_2\text{NMe}_2)]_2$ **2** and $[(\text{Bu}^t)_2\text{Al}(\mu\text{-OPr}^m)]_2$ **3** discussed above. This analogy has some precedent since we have previously shown by ¹⁷O NMR spectroscopy that aluminium and a proton have similar electronegativities with regard to oxygen.⁴

The unusual stability of **1** with respect to alkane elimination should be compared to the previous reports that reaction of aluminium alkyls with protic species is not significantly inhibited by being performed in strongly hydrogen-bonding solvents such as tetrahydrofuran (thf) or Et₂O.² Furthermore, consistent with this observation is that the reaction of $(\text{Bu}^t)_3\text{Al}(\text{NMe}_3)$ **4** with ethanol occurs below room temperature and results in the formation of $[(\text{Bu}^t)_2\text{Al}(\mu\text{-OEt})]_2$ **5** (see Experimental section).

As indicated above $(\text{Bu}^t)_3\text{Al}[\text{O}(\text{H})\text{CH}_2\text{CH}_2\text{CH}_2\text{NMe}_2]$ **1** decomposes slowly above 45 °C to yield **2** [equation (4)], and this reaction is readily observed by ¹H NMR spectroscopy. As would be expected, this alkane elimination reaction from **1** shows a first-order dependence with respect to **1** (see Experimental section and Table 4). The enthalpy of activation (ΔH^\ddagger) and entropy of activation (ΔS^\ddagger) were obtained from the appropriate Eyring plot (Fig. 6), from which the values of $132 \pm 4 \text{ kJ mol}^{-1}$ and $76 \pm 16 \text{ J K}^{-1} \text{ mol}^{-1}$ were calculated. The analogous reaction with $(\text{Bu}^t)_3\text{Al}[\text{O}(\text{D})\text{CH}_2\text{CH}_2\text{CH}_2\text{NMe}_2]$ (**1-d**, see Experimental section) shows a significant deuterium isotope effect; $\Delta H^\ddagger = 143 \pm 3 \text{ kJ mol}^{-1}$ and $\Delta S^\ddagger = 103 \pm 14 \text{ J}$

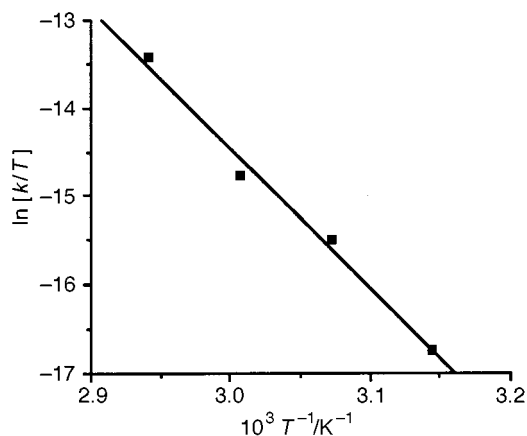
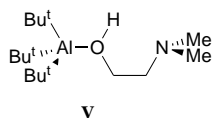


Fig. 6 Eyring plot for the determination of ΔH^\ddagger and ΔS^\ddagger for the alkane elimination reaction of $(\text{Bu}^t)_3\text{Al}[\text{O}(\text{H})\text{CH}_2\text{CH}_2\text{CH}_2\text{NMe}_2]$ **1** and its conversion into $[(\text{Bu}^t)_2\text{Al}(\mu\text{-OCH}_2\text{CH}_2\text{CH}_2\text{NMe}_2)]_2$ **2** ($R = 0.990$)



$\text{K}^{-1} \text{mol}^{-1}$. Unfortunately, while several kinetic studies have been previously reported for alkane elimination reactions involving AlR_3 and amines,²⁴ there are no data with which to compare our ΔH^\ddagger value.

The high ΔH^\ddagger is significantly larger than the values previously observed for similar $\text{O}-\text{H}\cdots\text{N}$ hydrogen bonds which are generally in the range $4\text{--}40 \text{ kJ mol}^{-1}$; although larger energies such as in KHF_2 (*ca.* 212 kJ mol^{-1}) are observed.²⁵ However, the positive value for ΔS^\ddagger and positive deuterium isotope effect are consistent with the breaking of the hydrogen bond and thus the formation of a non-hydrogen bonded intermediate (*cf.*, **V**) which would presumably then undergo rapid alkane elimination to yield $[(\text{Bu}^t)_2\text{Al}(\mu\text{-OCH}_2\text{CH}_2\text{CH}_2\text{NMe}_2)]_2$ **2**. It is also worth noting that the ΔH^\ddagger value determined for the conversion of **1** into **2** is significantly larger than the bond dissociation energies (BDEs) calculated for Lewis acid–base complexes of aluminium alkyls with neutral Lewis bases, *e.g.* $\text{Me}_3\text{Al}(\text{L})$ ($\text{L} = \text{Et}_2\text{O}$, $\text{BDE} = 84.6 \text{ kJ mol}^{-1}$; $\text{L} = \text{thf}$, $\text{BDE} = 95.8 \text{ kJ mol}^{-1}$; $\text{L} = \text{pyridine}$, $\text{BDE} = 115.3 \text{ kJ mol}^{-1}$).²⁶

We note that we have observed a similar structural dichotomy with regard to a hydroxide/oxide formulation in $(\text{Bu}^t)_2\text{Ga}(\text{C}_6\text{H}_4\text{NMe}_2\text{-}o)(\mu\text{-OH})\text{Ga}(\text{Bu}^t)[\text{C}_6\text{H}_4\text{N}(\text{O})\text{Me}_2\text{-}o]$.¹⁶ The $\text{Ga}-\text{O}(\text{H})$ bond distance [$1.868(8) \text{ \AA}$] was shorter than expected for a gallium hydroxide (*ca.* 2.00 \AA) but similar to that observed for gallium oxide ($1.87\text{--}1.89 \text{ \AA}$),²⁷ suggesting some component of the zwitterionic $\text{O}^-\cdots\text{H}-\text{N}^+$ form. However, in this case variable-temperature ^1H NMR spectroscopy allowed for the determination of the $\text{O}-\text{H}\cdots\text{N}$ hydrogen bond strength, $\Delta G^\ddagger = 57.3 \text{ kJ mol}^{-1}$. This may be compared to the value calculated for the conversion of **1** into **2** at 45°C of $107.8 \text{ kJ mol}^{-1}$.

Secondary amine complexes

While reactions of primary and secondary amines are ordinarily that of either a Brønsted or Lewis base, their reactions with $\text{Al}-\text{C}$ bonds are that of a Brønsted acid.²⁸ The isolation and unusual stability of compound **1** prompted our study of the isolation of diamine analogs. The reaction of $\text{Al}(\text{Bu}^t)_3$ with $\text{HN}(\text{Me})\text{CH}_2\text{CH}_2\text{CH}_2\text{NMe}_2$ and $\text{HN}(\text{Me})\text{CH}_2\text{CH}_2\text{NMe}_2$ yields the Lewis acid–base adducts $(\text{Bu}^t)_3\text{Al}[\text{NH}(\text{Me})\text{CH}_2\text{CH}_2\text{CH}_2\text{NMe}_2]$ **6** and $(\text{Bu}^t)_3\text{Al}[\text{NH}(\text{Me})\text{CH}_2\text{CH}_2\text{NMe}_2]$ **7**, respectively. Both compounds have been characterized spectroscopically (see Experimental section) and their molecular structures have been determined by X-ray crystallography. The variable-

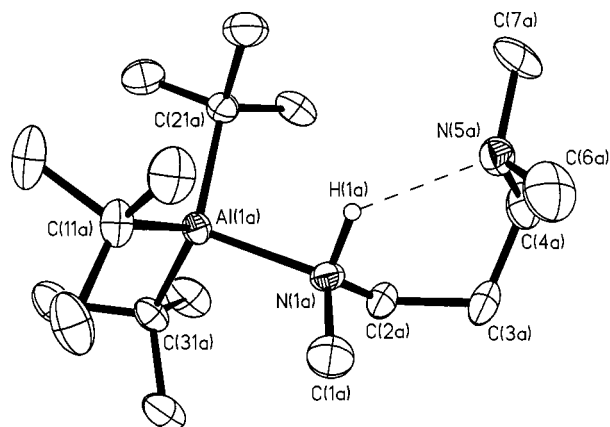


Fig. 7 Molecular structure of one of the crystallographically independent molecules of $(\text{Bu}^t)_3\text{Al}[\text{NH}(\text{Me})\text{CH}_2\text{CH}_2\text{CH}_2\text{NMe}_2]$ **6**. Thermal ellipsoids shown at the 20% level, and only the amine hydrogen is shown for clarity

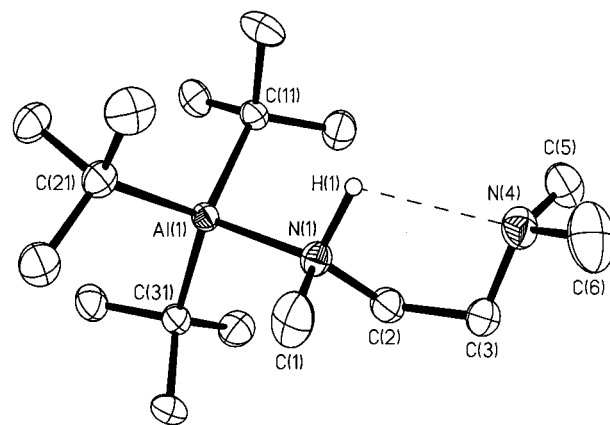


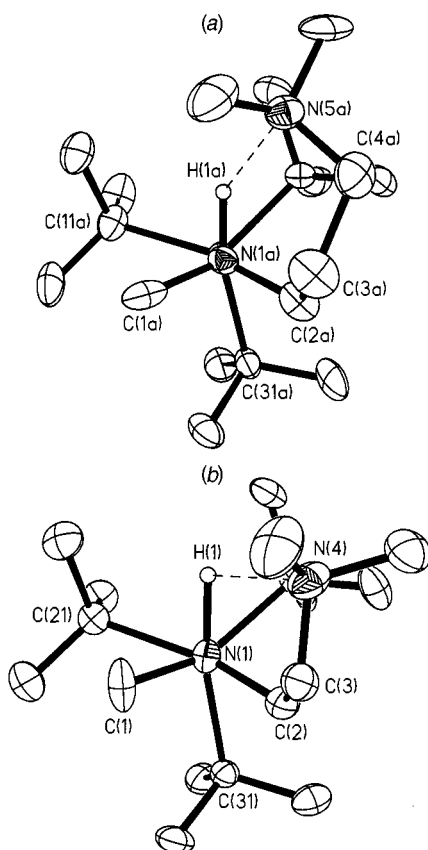
Fig. 8 Molecular structure of $(\text{Bu}^t)_3\text{Al}[\text{NH}(\text{Me})\text{CH}_2\text{CH}_2\text{NMe}_2]$ **7**. Thermal ellipsoids shown at the 20% level, and only the amine hydrogen is shown for clarity

temperature ^1H and ^{13}C NMR spectra of compound **6** shows no change over the temperature range -80°C to 25°C . Furthermore, unlike compound **1** both amine complexes are stable with respect to alkane elimination in solution up to 110°C for extended periods of time (2 days).

The molecular structures of $(\text{Bu}^t)_3\text{Al}[\text{NH}(\text{Me})\text{CH}_2\text{CH}_2\text{CH}_2\text{NMe}_2]$ **6** and $(\text{Bu}^t)_3\text{Al}[\text{NH}(\text{Me})\text{CH}_2\text{CH}_2\text{NMe}_2]$ **7** are shown in Figs. 7 and 8, respectively: selected bond lengths and angles are given in Table 5. Two independent molecules of compound **6** are present in the asymmetric unit, however, all bond lengths and angles are, within experimental error, the same between the two molecules. The $\text{Al}-\text{N}$ bond distances [$2.076(5)$ and $2.055(5) \text{ \AA}$] (**6**), $2.087(2) \text{ \AA}$ (**7**) are typical of amine Lewis acid–base complexes of aluminium. The diamine ligands adopt a configuration to allow hydrogen bonding between the secondary amine's hydrogen atom and the tertiary amine nitrogen. In both compounds the amine hydrogen atoms were located in the electron difference map and indicate the retention of the secondary amine/tertiary amine form rather than the zwitterionic amide⁻/ammonium⁺ form, *cf.*, **I** and **II**. This would be expected based on the relative basicity of secondary amide and tertiary amine. While the $\text{N}\cdots\text{N}$ distances are similar in compound **6** (2.96 \AA) to that in **7** (2.92 \AA), the $\text{N}-\text{H}\cdots\text{N}$ angle is significantly larger as a consequence of the six-membered *versus* five-membered ring, *i.e.*, 127° (**6**) *versus* 101° (**7**). As is observed for compound **1** the amine substituents in compounds **6** and **7** are staggered about the $\text{Al}-\text{N}$ bond [$\text{C}(31)-\text{Al}(1)-\text{N}(1)-\text{C}(2) = 39.4, 41.0^\circ$ (**6**) and $\text{C}(31)-\text{Al}(1)-\text{N}(1)-\text{C}(2) = 39.3^\circ$ (**7**)] with respect to the aluminium substituents, see Fig. 9.

Table 5 Selected bond lengths (Å) and angles (°) in (Bu^t)₃Al[NH(Me)CH₂CH₂CH₂NMe₂] **6** and (Bu^t)₃Al[NH(Me)CH₂CH₂NMe₂] **7**

	(Bu ^t) ₃ Al[NH(Me)CH ₂ CH ₂ CH ₂ NMe ₂]		
	Molecule A	Molecule B	(Bu ^t) ₃ Al[NH(Me)CH ₂ CH ₂ NMe ₂]
Al(1)–N(1)	2.076(5)	2.055(5)	2.087(2)
Al(1)–C(11)	2.023(7)	2.026(6)	2.049(2)
Al(1)–C(21)	2.028(6)	2.034(7)	2.046(2)
Al(1)–C(31)	2.050(7)	2.041(7)	2.034(2)
N(1)–Al(1)–C(11)	105.2(3)	104.3(2)	103.47(8)
N(1)–Al(1)–C(21)	103.6(2)	104.0(3)	105.26(8)
N(1)–Al(1)–C(31)	105.7(3)	106.7(3)	105.34(8)
C(11)–Al(1)–C(21)	113.0(3)	113.1(3)	112.84(9)
C(11)–Al(1)–C(31)	114.1(2)	113.3(3)	114.80(9)
C(21)–Al(1)–C(31)	114.0(3)	114.2(3)	113.75(9)

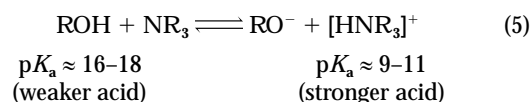
**Fig. 9** Structures of (a) (Bu^t)₃Al[NH(Me)CH₂CH₂CH₂NMe₂] **6** and (b) (Bu^t)₃Al[NH(Me)CH₂CH₂NMe₂] **7** viewed along their Al(1)–N(1) vectors. Thermal ellipsoids shown at the 20% level, and only the amine hydrogen atoms are shown for clarity.**Is protolytic alkane elimination from aluminium alkyls intra- or inter-molecular?**

It is widely observed that complexation of water to a transition metal increases its Brønsted acidity.²⁹ Similarly, an increased acidity of water upon complexation to aluminium alkyls has been inferred from the significant downfield shift of the water's proton resonance in the ¹H NMR spectra of R₃Al(OH₂) complexes as compared to 'free' water, see Table 6. Unfortunately, no quantitative data is available since the ¹H NMR data provides only a qualitative measure of the increased acidity of the water's protons. However, the isolation of compounds **1**, **6** and **7** allow the change in pK_a of Brønsted acid's proton upon complexation to aluminium to be estimated.

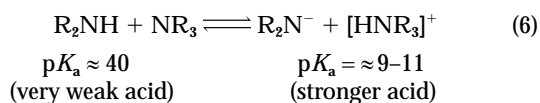
The pK_a of a primary alcohol has been reported to vary between 16–18,^{30,31} while for trialkyl ammonium salts pK_a ≈ 9–11.³² Thus, the equilibrium shown in equation (5)

Table 6 Proton NMR chemical shifts of water protons complexed to aluminium compounds

Compound	Solvent	δ (ppm)
H ₂ O	Et ₂ O	3.36
Me ₃ Al(OH ₂)	Et ₂ O	8.05 ^a
Et ₃ Al(OH ₂)	Et ₂ O	7.75 ^a
(Bu ^t) ₃ Al(OH ₂)	Et ₂ O	8.16 ^a
H ₂ O	thf	2.40
(mes) ₃ Al(OH ₂) ^b	thf	9.20 ^c
(Ph ₃ SiO) ₃ Al(OH ₂)	thf	3.86 ^d

^a Ref. 2. ^b mes = Mesityl. ^c Ref. 3. ^d Ref. 4.

lies well to the left. Based upon the structural characterization of (Bu^t)₃Al[O(H)CH₂CH₂CH₂NMe₂] **1** it appears that upon complexation of the alcohol moiety to aluminium this equilibrium moves significantly to the right, which necessitates a decrease in the pK_a of at least 7 units. In contrast, retention of the secondary amine/tertiary amine formulation in the structures of (Bu^t)₃Al[NH(Me)CH₂CH₂CH₂NMe₂] **6** and (Bu^t)₃Al[NH(Me)CH₂CH₂NMe₂] **7**, suggests that the pK_a of the secondary amine while possibly decreased upon co-ordination to aluminium is not sufficiently changed to overcome the large acidity difference shown in equation (6), *i.e.*, a decrease in pK_a of

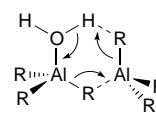
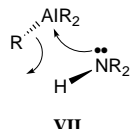
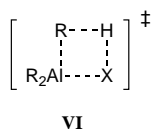


about 30 is not observed/possible. Based upon these we propose that upon complexation of a protic Lewis base (*e.g.*, ROH, R₂NH, *etc.*) to aluminium the α-proton exhibits an increase in Brønsted acidity discerned by a decrease in pK_a of about 7. We note that this activation of the co-ordinated ligand by increasing the formal positive charge on the α-substituent is analogous to the activation of organic carbonyls towards alkylation and/or reduction by aluminium alkyls.³³

It has been commonly assumed that the elimination-condensation reaction sequence [equation (1)] that occurs between an aluminium-alkyl and Brønsted acid (HX) proceeds *via* the prior formation of a Lewis acid–base adduct from which the elimination reaction occurs [equation (7)]. A concerted

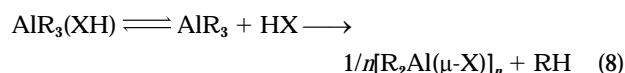
$$\text{AlR}_3 + \text{HX} \longrightarrow \text{AlR}_3(\text{XH}) \longrightarrow 1/n[\text{R}_2\text{Al}(\mu\text{-X})]_n + \text{RH} \quad (7)$$

intramolecular elimination possibly *via* a planar four-centered transition state (**VI**) is therefore proposed.³⁴ The differences in reactivity of various Brønsted acids was rationalized in terms of the acidity of the proton in the adduct molecule. Furthermore,



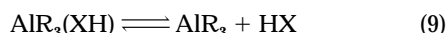
an intramolecular elimination reaction [equation (7) *via* VI] would be promoted by the increase in the acidity of the complexed species compared to the uncomplexed Brønsted acid.

In direct contrast to this proposal, Beachley *et al.*³⁵ demonstrated (for the reaction of aluminium alkyls and amines) that while a Lewis acid–base adduct is formed, the important step for the elimination–condensation reaction is a prior dissociation of the adduct [equation (8), where X = NR₂]. Recombination of

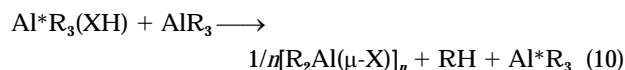


the monomeric aluminium compound and the amine with the appropriate orientation results in elimination *via* a four-centered S_Ei (substitution, electrophilic, internal) mechanism (VII).³⁶ The formation of a stable aluminium–amine adduct was found to be a ‘dead-end’ path for alkane elimination. It is not obvious however, why the Brønsted acid should react once uncomplexed from aluminium since it is at its most active (acidic) when complexed.

The contradictory nature of these proposed mechanisms prompts our suggestion of an alternative that is consistent with all the observed data. Therefore, we propose that the formation of the Lewis acid–base adduct activates the α-proton by increasing its acidity; measured by a decrease in its pK_a of about 7. However, intramolecular elimination does not occur due to the severe distortion that would be required to provide a geometry for a concerted four-membered transition state (VI). Instead, adduct dissociation yields ‘free’, but relatively unreactive, Brønsted acid and ‘free’ AlR₃, equation (9). This



uncomplexed AlR₃ reacts directly with another molecule of the activated complex, Al*R₃(XH), resulting in an intermolecular elimination–condensation reaction, equation (10). Hence, the



rate-determining step involves adduct dissociation, but the reactive species is the activated complex, Al*R₃(XH). The intermolecular reaction explains the exclusive formation of compound 2 when 2 equivalents of Al(Bu^t)₃ are reacted with HOCH₂CH₂CH₂NMe₂, *i.e.* equation (3).

Such a mechanism would also explain the decreased reactivity with respect to alkane elimination of aluminium *tert*-butyl derivatives *versus* the isobutyl, ethyl, or methyl analogs. The former does not allow for the formation of alkyl bridges that would stabilize a six-membered transition state, *e.g.* VIII for the reaction of AlR₃ with H₂O.

Conclusion

We have shown that stable alcohol and secondary amine co-ordination complexes of aluminium trialkyl compounds may be isolated through the application of intramolecular hydrogen bonding to a tertiary amine. While the retention of the secondary amine/tertiary amine form appears to be observed for the co-ordination of HN(Me)(CH₂)_nNMe₂ (*n* = 2 or 3), the zwitterionic alkoxide /ammonium⁺ form appears to predominate in the complex of HOCH₂CH₂CH₂NMe₂. Furthermore, the hydrogen-bonded hydrogen resembles an aluminium center with regard to observed electronegativity about oxygen. Thus,

the co-ordinated alcohol may actually be described as a bridging alkoxide, ‘Al(μ-OR)H’. These results suggest that a similar approach may be suitable for the isolation of amino acid complexes of aluminium alkyls.

The enhancement in the stability of Lewis acid–base complexes, between aluminium alkyls and protic moieties, through strong intramolecular hydrogen bonding, and the ability to investigate the subsequent kinetics of the alcoholysis reaction offers the possibility to undertake a comparative study of the protonolysis of Al–X bonds in a wide range of systems. In particular, the observation³⁷ that a rigid five-co-ordinate aluminium amide undergoes hydrolysis suggests that the traditional view of ligand dissociation from a Lewis acid–base complex may be incorrect.

We have proposed that the elimination–condensation reaction between an aluminium alkyl and a Brønsted acid occurs *via*: (a) activation of the Brønsted acid by formation of the Lewis acid–base adduct, (b) adduct dissociation to liberate ‘free’ aluminium alkyl, and (c) reaction of the activated Brønsted acid with ‘free’ aluminium alkyl. We are continuing our investigation of this proposed mechanism.

Experimental

All operations were carried out under an inert atmosphere using Schlenk techniques or VAC inert atmosphere dry box. Mass spectra were obtained on a Finnigan MAT 95 mass spectrometer operating with an electron beam energy of 70 eV ($\approx 1.1215 \times 10^{-17}$ J) for electron impact (EI) mass spectra. Infrared spectra (4000–400 cm⁻¹) were obtained using a Nicolet Magna 760 FT-IR infrared spectrometer; the samples were prepared as mulls on KBr plates. The NMR spectra were obtained on Bruker AM-250 and AM-300 spectrometers using (unless otherwise stated) C₆D₆ solutions. Chemical shifts are reported relative to internal solvent resonances (¹H and ¹³C), and external [Al(H₂O)₆]³⁺ (²⁷Al). Elemental analysis were performed using a Perkin-Elmer Magna 400 ICP atomic emission spectrometer. All compounds were digested in nitric acid to enable analysis. *Caution: digestion of organoaluminium compounds in acidic solutions should be undertaken with care.* The synthesis of Al(Bu^t)₃ was performed according to a literature method.³⁸ The compounds HOCH₂CH₂CH₂NMe₂, NH(Me)CH₂CH₂CH₂NMe₂ and NH(Me)CH₂CH₂CH₂NMe₂ were commercial samples and were used without further purification.

Syntheses

(Bu^t)₃Al[O(H)CH₂CH₂CH₂NMe₂] 1. To a hexane solution (40 cm³) of Al(Bu^t)₃ (1.6 g, 8.1 mmol), cooled to –78 °C, was added a hexane (20 cm³) solution of HOCH₂CH₂CH₂NMe₂ (0.84 g, 8.1 mmol). The reaction was warmed to room temperature and stirred overnight. The solution was filtered, concentrated, and cooled to –23 °C. Yield: 57%. M.p. 84–87 °C. IR (cm⁻¹): 3339w (br), 3076w (br), 1353m, 1303w, 1171s, 1081s, 1000w, 926w. ¹H NMR (C₆H₆): δ 3.92 [2 H, t, J(H–H) = 5.3, OCH₂], 1.67 [2 H, t, J(H–H) = 5.4, OCH₂CH₂CH₂], 1.43 (6 H, s, NCH₃), 1.40 [27 H, s, C(CH₃)₃], 0.86 [2 H, tt, J(H–H) = 5.4, J(H–H) = 5.3 Hz, OCH₂CH₂]. ¹³C NMR (C₆D₆): δ 66.8 (OCH₂), 60.6 (OCH₂CH₂CH₂), 43.2 (NCH₃), 33.7 [C(CH₃)₃], 24.0 (OCH₂CH₂). ²⁷Al NMR (C₆H₅Me–C₆D₆): δ 144 (ν₂ = 3153 Hz).

DOCH₂CH₂CH₂NMe₂. To an Et₂O (50 cm³) solution of HOCH₂CH₂CH₂NMe₂ (20 cm³, 0.167 mol) was added Bu^tLi

(100 cm³, 0.17 mol, 1.7 M in hexane) at -78 °C. The reaction was stirred for 30 min, reduction in volume and cooling (-15 °C for 16 h) resulted in the precipitation of LiOCH₂CH₂CH₂NMe₂ which was filtered off and dried. The lithium compound LiOCH₂CH₂CH₂NMe₂ (1.5 g, 13.7 mmol) was subsequently suspended in degassed Et₂O (50 cm³) and D₂O (0.25 cm³, 13.7 mmol) was syringed into the solution. The reaction mixture was stirred for 1 h. The solution was filtered and the ether was removed under a stream of nitrogen leaving a quantitative yield of colorless liquid. ¹H NMR (C₆D₆): δ 3.74 [2 H, t, *J*(H-H) = 5.0, OCH₂], 2.13 (2 H, br m, OCH₂CH₂CH₂), 1.88 [6 H, t, *J*(H-D) = 2.5 Hz, N(CH₃)₂], 1.40 (2 H, br m, OCH₂CH₂).

(Bu^t)₃Al[O(D)CH₂CH₂CH₂NMe₂] 1-d₁. Prepared as for compound **1** using Al(Bu^t)₃ (0.8 g, 4.0 mmol) and DOCH₂CH₂NMe₂ (0.55 g, 5.3 mmol). Yield 72%. IR (cm⁻¹): 2677m, 1716s (br), 1350m, 1304w, 1167s, 1113m, 1078s, 943m. ¹H NMR (C₆D₆): δ 3.90 [2 H, t, *J*(H-H) = 5.3, OCH₂], 1.61 [2 H, t, *J*(H-H) = 5.4 Hz, OCH₂CH₂CH₂], 1.42 [27 H, s, C(CH₃)₃], 1.39 [6 H, s, N(CH₃)₂], 0.83 (2 H, m, OCH₂CH₂). ¹³C NMR (C₆D₆): δ 66.9 (OCH₂), 60.6 (OCH₂CH₂CH₂), 43.2 [N(CH₃)₂], 33.7 [C(CH₃)₃], 24.2 (OCH₂CH₂).

(Bu^t)₂Al(μ-OCH₂CH₂CH₂NMe₂)₂ 2. To a hexane solution (40 cm³) of Al(Bu^t)₃ (2.00 g, 10.08 mmol), cooled to -78 °C, was added a hexane (20 cm³) solution of HOCH₂CH₂CH₂NMe₂ (0.60 cm³, 5.06 mmol). The reaction was warmed to room temperature and stirred overnight. The solution was filtered, concentrated, and cooled (-22 °C). Several crops of colorless crystals were collected by filtration and subsequent recoling of the filtrate. Yield: 72%. M.p. 143–145 °C [Found (Calc.): Al, 11.4 ± 0.03% (11.1%)]. Mass spectrum (EI, %): *m/z* 429 (2M⁺ - Bu^t, 100), 186 (M⁺ - Bu^t, 26), 86 [(CH₂)₃NMe₂, 73], 57 (Bu^t, 82). IR (cm⁻¹): 2788s, 1259s, 1184m, 1154m, 1085s (br), 1022s (br), 965m, 807s, 639m, 586m. ¹H NMR (C₆D₆): δ 3.98 [4 H, t, *J*(H-H) = 8.1, OCH₂], 1.98 [4 H, t, *J*(H-H) = 7.1 Hz, OCH₂CH₂CH₂], 1.97 (12 H, s, NCH₃), 1.82 (4 H, m, OCH₂CH₂), 1.26 [36 H, s, C(CH₃)₃]. ¹³C NMR (C₆D₆): δ 32.4 [C(CH₃)₃], 33.6 (OCH₂CH₂), 45.6 [N(CH₃)₂], 55.9 (OCH₂CH₂CH₂), 64.9 (OCH₂). ²⁷Al NMR (C₆H₅Me-C₆D₆): δ 143 (w₁ = 4400 Hz).

(Bu^t)₂Al(μ-OPrⁿ)₂ 3. A hexane solution (100 cm³) of Al(Bu^t)₃ (1.0 g, 5.0 mmol) was cooled to -78 °C, and freshly distilled HOCH₂CH₂CH₃ (0.3 g, 5.0 mmol) added by syringe. The mixture was then left to warm to room temperature as it stirred overnight. After filtering, concentrating, and cooling the solution to -23 °C, colorless crystals were collected by filtration. Yield: 42%. M.p. 248–250 °C (sublimes). Mass spectrum (chemical ionization, CH₄, %): *m/z* 343 (M⁺ - Bu^t, 100). IR (cm⁻¹): 2699m, 1358s, 1309m, 1260w, 1184m, 1045s, 1000s, 935s, 899s. ¹H NMR (C₆D₆): δ 3.64 [4 H, t, *J*(H-H) = 7.7, OCH₂], 1.59 [4 H, m, *J*(H-H) = 7.7, *J*(H-H) = 7.4, OCH₂CH₂], 1.21 [36 H, s, C(CH₃)₃], 0.53 [6 H, t, *J*(H-H) = 7.4 Hz, OCH₂CH₂CH₂]. ¹³C NMR (C₆D₆): δ 67.7 (OCH₂), 32.4 [C(CH₃)₃], 27.5 (OCH₂CH₂), 9.8 (OCH₂CH₂CH₃). ²⁷Al NMR (C₆H₅Me-C₆D₆): δ 146 (w₁ = 4300 Hz).

(Bu^t)₃Al(NMe₂) 4. Tri-*tert*-butylaluminium (0.8 g, 4.0 mmol) was dissolved in degassed hexane (ca. 40 cm³) and cooled to -78 °C. Trimethylamine (ca. 0.5 cm³, 5.5 mmol) was then condensed into the cooled solution. The mixture was then allowed to warm to room temperature as it stirred overnight. All the volatiles were removed under vacuum and the residue sublimed. Further purification was by recrystallization from hexane at -23 °C. Yield: 34%. Mass spectrum (EI, %): *m/z* 259 (M⁺ + 1, 4), 198 (M⁺ - NMe₂, 8), 141 [Al(Bu^t)₂N, 17], 57 (Bu^t, 100), 41 (AlN, 65). ¹H NMR (C₆D₆): δ 1.87 [9 H, s, N(CH₃)₃], 1.23

[27 H, s, C(CH₃)₃]. ¹³C NMR (C₆D₆): δ 49.8 [N(CH₃)₃], 33.8 [C(CH₃)₃].

(Bu^t)₃Al(μ-OEt)₂ 5. The compound (Bu^t)₃Al(NMe₂) (0.1 g, 0.39 mmol) was dissolved in degassed hexane (ca. 100 cm³) and cooled to -78 °C. Freshly distilled HOCH₂CH₃ (22 μl, 0.39 mmol) was added *via* syringe. The mixture was then allowed to warm to room temperature as it stirred overnight. The solvent and all volatiles were removed under vacuum and the residue recrystallised from hexane at -23 °C. Yield: 55%. Mass spectrum (EI, %): *m/z* 315 (2M⁺ - Bu^t, 100), 259 (2M⁺ - 2 Bu^t, 25). ¹H NMR (C₆D₆): δ 3.56 [4 H, q, *J*(H-H) = 7.3, OCH₂], 1.17 [36 H, s, C(CH₃)₃], 0.98 [6 H, t, *J*(H-H) = 7.3 Hz, OCH₂CH₃]. ¹³C NMR (C₆D₆): δ 61.2 (OCH₂), 32.3 [C(CH₃)₃], 19.2 (OCH₂CH₃).

(Bu^t)₃Al[NH(Me)CH₂CH₂CH₂NMe₂] 6. To a hexane solution (50 cm³) of Al(Bu^t)₃ (3.4 g, 17.1 mmol), cooled to -78 °C, was added Me₂NCH₂CH₂CH₂NH(Me) (2.1 g, 18.1 mmol). The mixture was then allowed to warm to room temperature and stirred overnight. After filtration, concentration and cooling the solution to -22 °C, the pale yellow crystals formed were collected by filtration. Several crops were obtained by subsequent recoling of the filtrate. Yield: 67%. M.p. 61–63 °C. Mass spectrum (EI, %): *m/z* 257 (M⁺ - Bu^t, 22), 198 (M⁺ - Bu^t - CH₂NMe₂, 10), 141 (M⁺ - 2 Bu^t - CH₂NMe₂, 28), 57 (Bu^t, 100). IR (cm⁻¹): 3089s ν(N-H), 2691s, 1358m, 1292s, 1246m, 1163m, 1078m, 1038s, 986m, 939s, 809s, 760s, 462s (br). ¹H NMR (C₆D₆): δ 5.04 (1 H, br s, NH), 3.23 [2 H, t, *J*(H-H) = 8.1, NCH₂], 2.13 [3 H, d, *J*(H-H) = 6.1 Hz, NCH₃], 2.07 (2 H, m, NCH₂), 1.72 [6 H, s, N(CH₃)₂], 1.32 [27 H, s, C(CH₃)₃], 0.49 (2 H, m, NCH₂CH₂). ¹³C NMR (C₆D₆): δ 59.9 (NCH₂), 52.9 (NCH₂), 45.9 [N(CH₃)₂], 35.4 (NCH₃), 33.7 [C(CH₃)₃], 20.4 [NCH₂CH₂], 18.2 [C(CH₃)₃]. ²⁷Al NMR (C₆H₅Me-C₆D₆): δ 150 (w₁ = 3530 Hz).

(Bu^t)₃Al[NH(Me)CH₂CH₂NMe₂] 7. Prepared as for compound **6** using Al(Bu^t)₃ (4.0 g, 20.2 mmol) and Me₂NCH₂CH₂NH(Me) (2.58 g, 25.2 mmol). Yield: 38%. M.p. 59–62 °C. Mass spectrum (EI, %): *m/z* 243 (M⁺ - Bu^t, 22), 198 (M⁺ - Bu^t - NMe₂, 14), 185 (M⁺ - 2 Bu^t, 8), 141 (M⁺ - 2 Bu^t - NMe₂, 30), 57 (Bu^t, 100). IR (cm⁻¹): 3202m ν(N-H), 1358s, 1288s, 1208s, 1179s (br), 1058s, 944s, 931s, 769s, 562s (br). ¹H NMR (C₆D₆): δ 3.05 (2 H, m, NCH₂), 2.05 [3 H, d, *J*(H-H) = 6.2 Hz, NCH₃], 1.99 (2 H, m, NCH₂), 1.79 [6 H, s, N(CH₃)₂], 1.30 [27 H, s, C(CH₃)₃]. ¹³C NMR (CDCl₃): δ 53.6 (NCH₂), 48.0 (NCH₂), 46.0 [N(CH₃)₂], 34.6 (NCH₃), 33.7 [C(CH₃)₃]. ²⁷Al NMR (C₆H₅Me-C₆D₆): δ 148 (w₁ = 4199 Hz).

Kinetic studies

A series of samples of (Bu^t)₃Al[O(H)CH₂CH₂CH₂NMe₂] **1** was accurately weighed (±0.005 g) into a series of 5 mm NMR tubes. To each tube was added an accurately weighed 0.5 cm³ aliquot of C₆D₆, the mass of solution determined, and thus the concentration of compound **1**. All of the samples were heated to the appropriate temperature within the NMR spectrometer, and a series of ¹H NMR spectra was collected every 10 min for up to 10 h. The temperature of the NMR spectrometer probe was calibrated using the chemical shifts of ethylene glycol.³⁹ The relative integration of the *tert*-butyl proton resonances of the reactant and product was used to determine the rate of reaction at each of four temperatures. Independent reactions were run at 326 K (0.132 and 0.084 M) in order to confirm the first-order nature of the reaction. The first order rate constants (*k*₁) were determined from a plot of -ln[**1**] *versus* time. Selected kinetic data are given in Table 4 and are used for the Eyring plot in Fig. 6.

Table 7 Summary of X-ray diffraction data

Compound	(Bu ^t) ₃ Al[O(H)CH ₂ CH ₂ CH ₂ NMe ₂] 1	[(Bu ^t) ₂ Al(μ-OCH ₂ CH ₂ CH ₂ NMe ₂) ₂] 2	[(Bu ^t) ₂ Al(μ-OPr ^{<i>i</i>}) ₂] 3	(Bu ^t) ₃ Al[NH(Me)CH ₂ CH ₂ CH ₂ NMe ₂] 6	(Bu ^t) ₃ Al[NH(Me)CH ₂ CH ₂ NMe ₂] 7
Empirical formula	C ₁₇ H ₄₀ AlNO	C ₂₆ H ₆₀ Al ₂ N ₂ O ₂	C ₂₂ H ₅₀ Al ₂ O ₂	C ₁₈ H ₄₃ AlN ₂	C ₁₇ H ₄₁ AlN ₂
<i>M</i>					
Crystal size/mm	0.34 × 0.37 × 0.41	0.22 × 0.26 × 0.30	0.09 × 0.11 × 0.12	0.22 × 0.25 × 0.28	0.23 × 0.31 × 0.45
Crystal system	Monoclinic	Triclinic	Triclinic	Monoclinic	Monoclinic
Space group	<i>P</i> 2 ₁ / <i>c</i>	<i>P</i> 1	<i>P</i> 1	<i>P</i> 2 ₁ / <i>c</i>	<i>P</i> 2 ₁ / <i>c</i>
<i>a</i> /Å	12.601(1)	8.5988(7)	8.548(2)	15.326(2)	8.967(1)
<i>b</i> /Å	9.900(1)	9.834(1)	8.933(1)	17.354(2)	11.693(1)
<i>c</i> /Å	16.984(3)	11.045(1)	9.9449(9)	18.032(2)	20.032(2)
<i>α</i> /°		64.159(9)	99.638(9)		
<i>β</i> /°	92.32(1)	76.175(8)	103.71(1)	113.285(8)	92.748(8)
<i>γ</i> /°		78.055(8)	107.29(1)		
<i>U</i> /Å ³	2116.9(5)	810.6(2)	681.0(2)	4405.3(8)	2098.0(4)
<i>Z</i>	4	1	1	8	4
<i>D_c</i> /g cm ⁻³	0.946	0.997	0.977	0.948	0.951
<i>μ</i> /cm ⁻¹	0.91	1.06	1.14	0.87	0.90
<i>TK</i>	298	298	298	298	298
2θ range/°	3.0–44.0	2.0–50.0	3.0–44.0	3.0–44.0	3.0–45.0
No. data collected	2905	2853	1666	5859	3082
No. independent data	2771	2853	1666	5624	2887
No. observed data	1156 ($ F_o > 6.0\sigma F_o $)	2202 ($ F_o > 6.0\sigma F_o $)	576 ($ F_o > 6.0\sigma F_o $)	2376 ($ F_o > 6.0\sigma F_o $)	1711 ($ F_o > 6.0\sigma F_o $)
Weighting scheme, <i>w</i> ⁻¹	0.04 ($ F_o $) ² + $\sigma(F_o)$ ²	$\sigma^2(F_o)$	0.04 ($ F_o $) ² + $\sigma(F_o)$ ²	0.04 ($ F_o $) ² + $\sigma(F_o)$ ²	0.04 ($ F_o $) ² + $\sigma(F_o)$ ²
<i>R</i>	0.0826	0.0606	0.0874	0.0578	0.0297
<i>R'</i>	0.1062	0.0610	0.0926	0.0582	0.0413
Largest difference peak e Å ⁻³	0.32	0.44	0.39	0.21	0.15

Crystallographic studies

Crystals of compounds **1–3**, **6** and **7** were sealed in a glass capillary under argon and mounted on the goniometer of an Enraf-Nonius CAD-4 automated diffractometer. Data collection and cell determinations were performed in a manner previously described.¹⁵ The location of the majority of non-hydrogen atoms were obtained by using either SIR (for **3**)⁴⁰ or SHELXS 86 (for **1**, **2**, **6**, **7**)⁴¹ while the remaining atomic coordinates were determined through the generation of Fourier difference maps using MOLEN.⁴² Disorder was noted in both the propoxide chain (slinky-type)²¹ and the *tert*-butyl groups of compound **3**. Refinement of site occupancy converged at a ratio of 2:1. The high thermal motion present in compound **1** also implies such a disorder. This could not be resolved, however. All non-hydrogen atoms were treated with anisotropic thermal parameters, except in compound **3**, for which sufficient data were available to treat only the Al and O atoms in this fashion. Organic hydrogen atoms were included with fixed thermal parameters and constrained to 'ride' upon the appropriate atoms [$d(\text{C-H}) = 0.95 \text{ \AA}$]. A summary of cell parameters, data collection, and structure solution is given in Table 7. Scattering factors were taken from ref. 43.

CCDC reference number 186/652.

Acknowledgements

Financial support for this work is provided by the Robert A. Welch Foundation.

References

- 1 J. J. Eisch, in *Comprehensive Organometallic Chemistry*, eds. G. Wilkinson, F. G. A. Stone and E. W. Abel, Pergamon Press, Oxford, 1986, vol. 1, ch. 6.
- 2 M. Boleslawski and J. Serwatowski, *J. Organomet. Chem.*, 1983, **255**, 269.
- 3 J. Storre, A. Klemp, H. W. Roesky, H.-G. Schmidt, M. Noltemeyer, R. Fleisher and D. Stalke, *J. Am. Chem. Soc.*, 1996, **118**, 1380.
- 4 A. W. Ablett, A. C. Warren and A. R. Barron, *Can. J. Chem.*, 1992, **70**, 771.
- 5 M. Taghiof, D. G. Hendershot, M. Barber and J. P. Oliver, *J. Organomet. Chem.*, 1992, **431**, 271.
- 6 M. D. Healy, J. W. Ziller and A. R. Barron, *Organometallics*, 1991, **10**, 597.
- 7 M. D. Healy, M. B. Power and A. R. Barron, *Coord. Chem. Rev.*, 1994, **130**, 63.
- 8 G. H. Robinson, W. T. Pennington, B. Lee, M. F. Self and D. C. Hrnčir, *Inorg. Chem.*, 1991, **30**, 809.
- 9 S. Ahrland, J. Chatt and N. R. Q. Davis, *Rev. Chem. Soc.*, 1958, **12**, 265; G. Schwarzenbach and M. Schellenberg, *Helv. Chim. Acta*, 1965, **48**, 28; G. Schwarzenbach, *Adv. Inorg. Chem. Radiochem.*, 1961, **3**, 257.
- 10 H. Schumann, M. Frick, B. Heymer and F. Girgsdies, *J. Organomet. Chem.*, 1996, **512**, 117.
- 11 D. A. Wierda and A. R. Barron, *Polyhedron*, 1989, **8**, 831.
- 12 C. N. McMahon and A. R. Barron, *J. Chem. Crystallogr.*, 1997, **27**, 171.
- 13 C. J. Harlan, S. G. Bott and A. R. Barron, *J. Am. Chem. Soc.*, 1995, **117**, 6465.
- 14 J. P. Oliver and R. Kumar, *Polyhedron*, 1990, **9**, 409.
- 15 M. R. Mason, J. M. Smith, S. G. Bott and A. R. Barron, *J. Am. Chem. Soc.*, 1993, **115**, 4971.
- 16 C. N. McMahon, S. G. Bott and A. R. Barron, *Polyhedron*, 1997, in the press.
- 17 R. Taylor and O. Kennard, *Acc. Chem. Res.*, 1984, **17**, 320.
- 18 C. L. Aitken and A. R. Barron, *J. Chem. Crystallogr.*, 1996, **26**, 293.
- 19 *Coordination Chemistry of Aluminum*, ed. G. H. Robinson, VCH, New York, 1993.
- 20 C. N. McMahon, J. A. Francis and A. R. Barron, *J. Chem. Crystallogr.*, 1997, **27**, 167.
- 21 C. L. Aitken and A. R. Barron, *J. Chem. Crystallogr.*, 1996, **26**, 297.
- 22 F. A. Cotton and G. Wilkinson, *Advanced Inorganic Chemistry*, Wiley, New York, 4th edn., 1980, p. 152.
- 23 R. Hoffmann, *Angew. Chem., Int. Ed. Engl.*, 1982, **21**, 711.
- 24 O. T. Beachley, jun. and L. Victoriano, *Inorg. Chem.*, 1986, **25**, 1948.
- 25 G. C. Pimentel and A. L. McClellan, *The Hydrogen Bond*, Freeman, San Francisco, CA, 1960; M. D. Joesten and L. J. Schaad, *Hydrogen Bonding*, Dekker, New York, 1974.
- 26 C. H. Henrickson, D. Duffy and D. P. Eyman, *Inorg. Chem.*, 1968, **7**, 1047.
- 27 C. C. Landry, C. J. Harlan, S. G. Bott and A. R. Barron, *Angew. Chem., Int. Ed. Engl.*, 1995, **34**, 1202 and refs. therein.
- 28 N. Davidson and H. C. Brown, *J. Am. Chem. Soc.*, 1942, **64**, 316.
- 29 C. F. Baes and R. E. Mesmer, *The Hydrolysis of Cations*, Wiley, New York, 1976; V. Baran, *Coord. Chem. Rev.*, 1971, **6**, 65.
- 30 P. Ballinger and F. A. Long, *J. Am. Chem. Soc.*, 1960, **82**, 795.
- 31 W. K. McEwen, *J. Am. Chem. Soc.*, 1936, **58**, 1124.
- 32 E. M. Arnett, *Prog. Phys. Org. Chem.*, 1963, **1**, 223; H. C. Brown, D. H. McDaniel and O. Häflinger, in *Determination of Organic Structures by Physical Methods*, eds. E. A. Braude and F. C. Nachod, Academic Press, New York, 1955.
- 33 M. B. Power, S. G. Bott, J. L. Atwood and A. R. Barron, *J. Am. Chem. Soc.*, 1990, **112**, 3446; M. B. Power, S. G. Bott, D. L. Clark, J. L. Atwood and A. R. Barron, *Organometallics*, 1990, **9**, 3086; M. B. Power, J. R. Nash, M. D. Healy and A. R. Barron, *Organometallics*, 1992, **11**, 1830.
- 34 G. E. Coates, M. L. H. Green and K. Wade, *Organometallic Compounds*, Methuen, London, 3rd edn., 1967, vol. 1, ch. 3; F. G. A. Stone, *Chem. Rev.*, 1958, **58**, 101.
- 35 O. T. Beachley, jun. and C. Tessier-Youngs, *Inorg. Chem.*, 1979, **18**, 3188; O. T. Beachley, jun., *Inorg. Chem.*, 1981, **20**, 2825.
- 36 M. H. Abraham and J. A. Hill, *J. Organomet. Chem.*, 1967, **7**, 11.
- 37 D. A. Atwood and D. Rutherford, 213rd ACS National Meeting, San Francisco, CA, 1997.
- 38 W. Uhl, *Z. Anorg. Allg. Chem.*, 1989, **570**, 37; H. Lehmkuhl, O. Olbrysch and H. Nehl, *Liebigs Ann. Chem.*, 1973, 708; H. Lehmkuhl and O. Olbrysch, *Liebigs Ann. Chem.*, 1973, 715.
- 39 A. L. van Geet, *Anal. Chem.*, 1968, **40**, 2227; H. J. Gordon and R. A. Ford, *The Chemists Companion*, Wiley, New York, 1972.
- 40 M. C. Burla, M. Carnalli, G. Cascarano, C. Giacovazzo, G. Polidori, R. Spagna and D. Viterbo, *J. Appl. Crystallogr.*, 1989, **22**, 389.
- 41 G. M. Sheldrick, *Acta Crystallogr., Sect. A*, 1990, **46**, 467.
- 42 MOLEN, An Interactive Structure Solution Procedure, Enraf-Nonius, Delft, 1990.
- 43 *International Tables for X-Ray Crystallography*, Kynoch Press, Birmingham, 1974, vol. 4, pp. 99, 149.

Received 11th May 1997; Paper 7/03222F